Culturing functional pancreatic islets on α5-laminins and curative transplantation to diabetic mice

Kristmundur Sigmundsson[a,†], Juha R.M. Ojala[b,†], Miina K. Öhman[a,‡], Anne-May Österholm[a,b,‡], Aida Moreno-Moral[a,‡], Anna Domogatskaya[b,‡,§], Li Yen Chong[a], Yang Sun[a], Xiaoran Chai[a], Joseph A.M. Steele[c], Benjamin George[a], Manuel Patarroyo[d], Ann-Sofie Nilsson[b], Sergey Rodin[b,‖], Sujoy Ghosh[a], Molly M. Stevens[c,e], Enrico Petretto[a] and Karl Tryggvason[a,b]

a - Cardiovascular and Metabolic Disorders Program, *Duke-NUS Medical School, Singapore*
b - Division of Matrix Biology, *Department of Medical Biochemistry and Biophysics, Karolinska Institutet, Stockholm, Sweden*
c - Division of Biomaterials and Regenerative Medicine, *Department of Medical Biochemistry and Biophysics, Karolinska Institutet, Stockholm, Sweden*
d - Department of Microbiology, *Tumor and Cell Biology, Karolinska Institutet, Stockholm, Sweden*
e - Department of Materials, *Department of Bioengineering and Institute for Biomedical Engineering, Imperial College London, Exhibition Road, London SW7 2AZ, UK*

Correspondence to Karl Tryggvason: *Cardiovascular and Metabolic Disorders Program, Duke-NUS Medical School, Singapore.* *karl.tryggvason@duke-nus.edu.sg*
https://doi.org/10.1016/j.matbio.2018.03.018

Abstract

The efficacy of islet transplantation for diabetes treatment suffers from lack of cadaver-derived islets, islet necrosis and long transfer times prior to transplantation. Here, we developed a method for culturing mouse and human islets *in vitro* on α5-laminins, which are natural components of islet basement membranes. Adhering islets spread to form layers of 1–3 cells in thickness and remained normoxic and functional for at least 7 days in culture. In contrast, spherical islets kept in suspension developed hypoxia and central necrosis within 16 h. Transplantation of 110–150 mouse islets cultured on α5-laminin-coated polydimethylsiloxane membranes for 3–7 days normalized blood glucose already within 3 days in mice with streptozotocin-induced diabetes. RNA-sequencing of isolated and cultured mouse islets provided further evidence for the adhesion and spreading achieved with α5-laminin. Our results suggest that use of such *in vitro* expanded islets may significantly enhance the efficacy of islet transplantation treatment for diabetes.

Introduction

Transplantation of pancreatic islets allows long-term effective and safe treatment for type 1 diabetes (T1D) patients [1], with the 5-year insulin independence rate of islet transplants being comparable with that of whole pancreas transplantation [2]. Islet transplantation is minimally invasive and confers less risks than transplantation of a whole pancreas, which requires major surgery and bears a risk of mortality [2,3]. Currently islet transplantation therapy is severely hampered by a shortage of donor material, alloimmune reactions, long donor-to-recipient transport times and compromised quality of transplanted islets. Although the combined need for islet transplantation therapy of T1D in the USA and UK was estimated to be 180,000, only 864 transplantations (islet or simultaneous islet and kidney) were carried out during 1999–2012 [4]. The main problems are that 2–5 donors may be required for obtaining sufficient amount of islets [1] and isolated islets in suspension tend to undergo necrosis [5].

In vivo, basement membranes (BM) constitute specialized sheet-like ECMs in the proximity of all organized cells. BMs are located immediately beneath

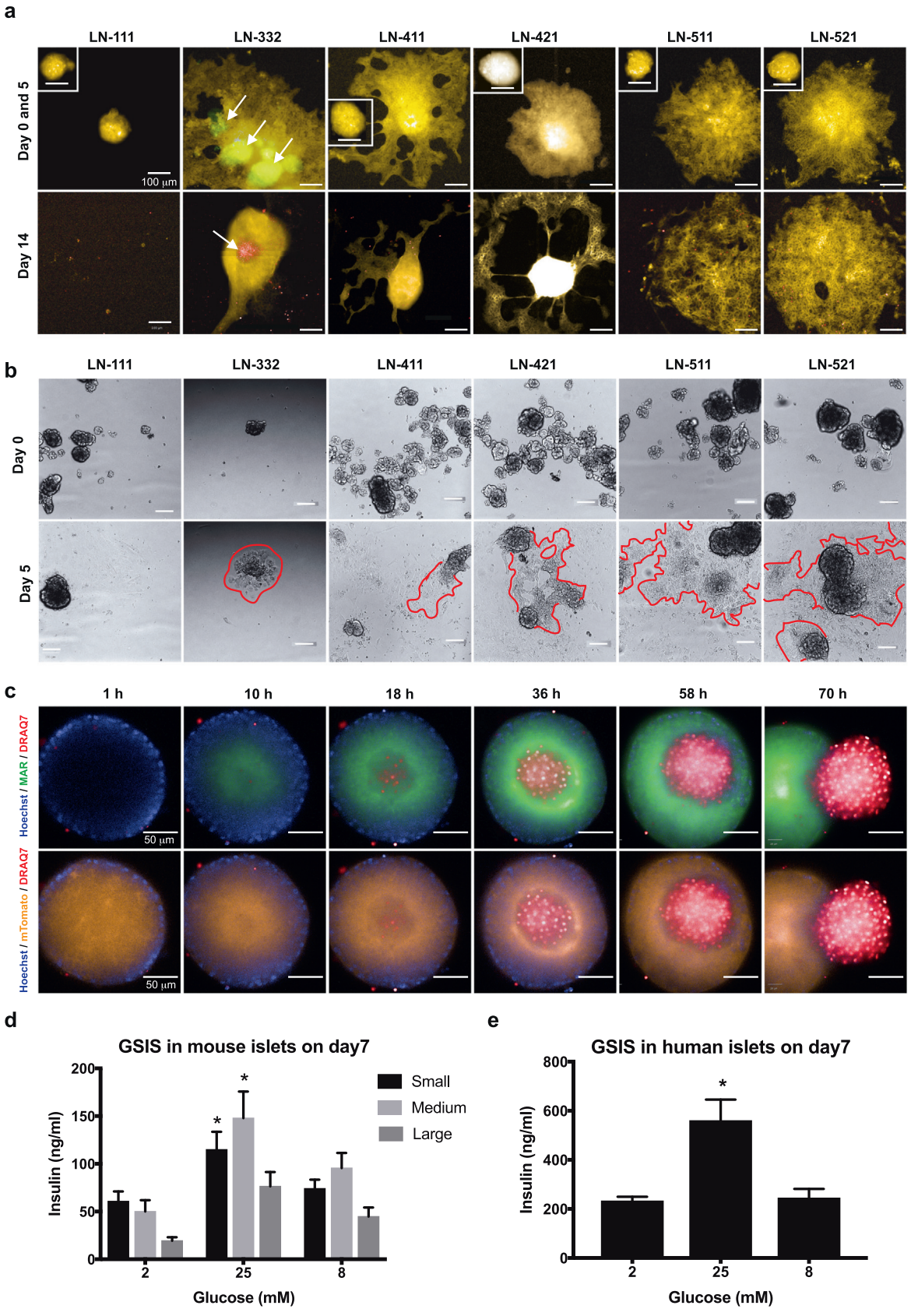

Fig. 1. (*legend on next page*)

endothelia and epithelia, or they surround individual cells, such as muscle fibers, adipocytes and axon bundles. In addition to laminins (LN), the BMs contain type IV and XVIII collagens and the proteoglycans, perlecan and agrin, as their main components [6–9]. Laminins (LN) are important components of BMs. They are trimeric protein complexes composed of three subunits, α-, β- and γ-chains, encoded by five, four and three distinct genes, respectively (*LAMA1–5, LAMB1–4, LAMC1–3*). So far, sixteen different laminin isoforms have been identified in higher organisms [6]. The laminins have been shown to influence cells in a cell-type specific manner, including stem cell differentiation [6,7]. We have previously shown that LN-411 and LN-511, produced by the islet endothelia, stimulate insulin secretion in mouse insulinoma cells [10]. Here, we show that physiologically relevant laminins can be used for culturing of functional pancreatic islets.

Results

Isolated islets maintain normoxia and functionality while spreading on LN-521

In order to explore if specific extracellular matrix (ECM) proteins support *in vitro* growth of pancreatic islets, we first investigated the repertoire of laminin isoforms found in islets of a non-human primate (*Macaca fascicularis*) to compare with previously published studies on mouse and human [6,10,11]. Monkey islets were found to contain laminin chains α4, α5, β1, β2 and γ1 (Suppl. Fig. 1). These can form LN-411, LN-421, LN-511 and LN-521 isoforms. In a capsule-like structure surrounding the islets, we detected α5-laminins only. Other laminins, including α1-3, β3 and γ2 were not detected (Suppl. Fig. 1). We plated isolated mouse and human islets on recombinant human laminins LN-411, LN-421, LN-511 and LN-521, to mimic the *in vivo* condition [11] (mouse: Fig. 1a and human: Fig. 1b, respectively). Islets on LN-111 adhered poorly and displayed limited spreading during the first 5 days in culture. By day 14, majority of islets plated on LN-111 were greatly diminished and appeared involuted (Fig. 1a, b, Suppl. Video 1a). Islets attached to LN-332, LN-411 and LN-421, but spreading was not extensive and between days 5-14, the islets started shrinking due to re-clustering followed by partial necrosis by day 14. In contrast, islets on LN-511 and LN-521 attached and spread effectively, with LN-521 providing slightly better attachment and expansion for the mouse (Fig. 1a). Similarly, the α5-laminins provided the most extensive spreading for human islets (Fig. 1b). Therefore, the rest of the experiments were performed with LN-521. Based on time-lapse analyses, mouse islets on LN-511 or LN-521 flattened from spheres into 1-3-cell layer sheets, heading towards a monolayer culture while maintaining cell-to-cell contacts (Fig. 1a, Suppl. Video 1b, Suppl. Fig. 2).

A suspension of isolated islets from mTomato mouse was placed in a medium, containing indicators for hypoxia (MAR) and necrosis (DRAQ7) (Fig. 1c, Suppl. Videos 2a and b). Hypoxia was observed already within a couple of hours, followed by necrosis of the central cell mass within 16 h (Fig. 1c), and subsequent expulsion of a necrotic core lacking the mTomato signal (Suppl. Videos 2a and b). In contrast, small and medium size islets cultured as spreading layers on LN-521 did not develop severe hypoxia or central necrosis under otherwise same conditions (Suppl. Fig. 2). To test for *in vitro* functionality of islets grown on LN-521, we measured glucose stimulated insulin secretion (GSIS) of islets after 3 and 7 days in culture. Except for large size mouse islets (diameter > 150 μm), both mouse (Fig. 1d and Suppl. Fig. 3a) and human (Fig. 1e) islets showed a physiological response to elevated glucose.

Transplantation of islets expanded on LN-521 rescues diabetes in mice

Isolated mouse islets were plated onto circular polydimethylsiloxane (PDMS) membranes coated with LN-521 and cultured for 3 or 7 days prior to transplantation (Suppl. Fig. 4a). Attachment and spreading of islets were equal on coated membranes and culture plates. Two membranes containing a total of 110–150 islets were placed under the kidney capsule, with islets facing the cortex (Suppl. Fig. 4a), of streptozotocin (STZ)-injected, hyperglycemic mice [12–14]. In total, 22 mice were transplanted (5 females and 17 males) and followed for 9 weeks post-operatively. A control group of STZ-injected, null-grafted male

Fig. 1. α5-laminins support survival and functionality of cultured mouse and human islets. (a) Spreading of mTomato mouse islets was followed from day 0–14. inserts (top left) provide the islets at time of plating (Day 0: for LN-332 arrows indicate three islets, whose initial forms and positions are shown overlaid in green). Formation of a necrotic core is indicated by DRAQ7, which is uptaken by nuclei (arrow to red nuclei). Scale bar 100 μm. (b) Spreading of human islets from day 0–5 is indicated by red curves surrounding the endocrine cell populations. Scale bar 100 μm. (c) Time-lapse of hypoxia induced necrosis occurring in an isolated mouse islet (diameter ≈ 150 μm); Hoechst (blue) for nuclei, MAR (green) for hypoxia, DRAQ7 (red) for nuclei of dying/dead cells, mTomato (orange) for viable cells. Scale bar 50 μm. (d) GSIS on mouse islets cultured for 7 days on LN-521. Islets sorted by size (μm, small: 70–100; medium: 100–150; large: 150–250) and plated in triplicates (n = 3 wells). Values: mean ± SEM. (e) GSIS on human islets cultured for 7 days on LN-521. Ten medium-sized islets per well (n = 5 wells). Values: mean ± SEM. * $p < 0.05$, for 2 mM *vs.* 25 mM within each size group, by pair-wise, 2-tailed *t*-test.

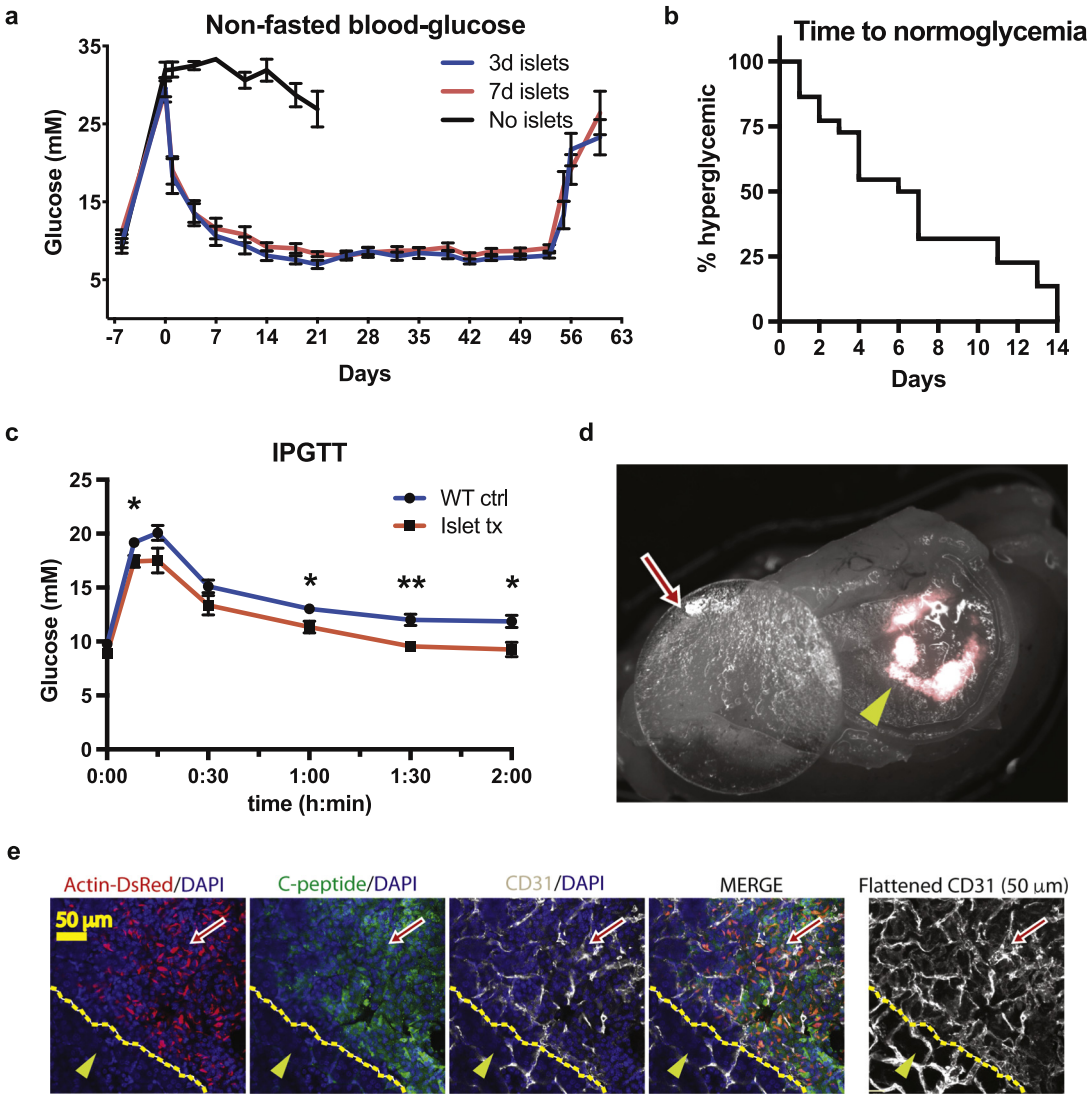

Fig. 2. Islets cultured on LN-521 display normal glucose responsiveness *in vivo*. (a) Non-fasted glucose levels were followed for 9 weeks in diabetic mice transplanted with syngeneic islets cultured on LN-521 for either 3 days (n = 12 mice) or 7 days (n = 10 mice). Control group of null-graft mice (n = 4) received membranes devoid of islets and were followed for three weeks. Streptozotocin was injected 7 days prior to transplantation (day 0). Nephrectomy was performed on day 53–56. Values: mean ± SEM. (b) Time to normoglycemia in transplanted mice (n = 22). (c) IPGTT performed to transplanted mice (n = 9) 6 weeks post-operation. Age-matched non-diabetic wild-type male mice (n = 7) were used as controls. Values: mean ± SEM. * $p < 0.05$, ** $p < 0.01$. (d) After nephrectomy, PDMS membrane was removed (red arrow). The fluorescent transplanted islets (yellow arrowhead) derived from Actin-DsRed transgenic mice engrafted to the kidney parenchyma. (e) Transplanted islets identified by Actin-DsRed fluorescence (red) within the area marked by a red arrow, separated from kidney parenchyma (yellow arrowhead) by a yellow dash line; DAPI (blue) for nuclei, C-peptide (green) for β-cells, CD31 (white) for endothelium. A 50 µm *Z*-stack of CD31 staining in the last panel. Scale bar 50 µm.

mice (n = 4) were transplanted with PDMS membranes devoid of islets and followed for three weeks (Fig. 2a). In the mice receiving islets, blood glucose normalized (≤11.5 mM, in two consecutive measurements) equally efficiently in mice treated with islets from 3 or 7 days cultures (Fig. 2a) and no differences was observed between sexes (Suppl. Fig. 3b). Normoglycemia was reached in 27% of mice already within 3 days and in 68% of mice within a week (Fig. 2b). By two weeks, all mice had reached normal glucose levels. Intraperitoneal glucose tolerance test (IPGTT) showed enhanced glucose clearance compared to wild-type control mice (Fig. 2c). Mice became hyperglycemic following nephrectomy of the graft-containing kidney at 8 weeks post-transplantation (Fig. 2a). Fluorescence detection of Actin-DsRed showed that the transplanted

islets had grown into the kidney cortex (Fig. 2d). Immunohistological stainings confirmed insulin production (C-peptide$^+$) and dense capillary network (CD31$^+$) within the grafts (Fig. 2e). No overlap of donor cells with CD31$^+$ cells was observed, indicating that vascularization originated from the host (Fig. 2e). Overall, these results show that transplantation of a relatively low number (110–150) of functional islets is sufficient to normalize hyperglycemia in a mouse model of T1D. This corresponds roughly to 4–5% of pancreatic islets of a normal mouse [15].

Integrin profile and transcriptomic analysis of spreading islets

To elucidate the involvement of potential adhesion receptors, we analyzed integrin expression in isolated (day 0) mouse islets using RNA sequencing (RNA-seq) analysis (Fig. 3a, Suppl. Table 1). This highlighted integrin β1 (*Itgb1*), αV (*Itgav*) and α6 (*Itga6*) as the most abundant transcripts (Fragments Per Kilobase of transcript per Million (FPKM) ≥ 50) amongst those proposed to specifically bind laminins [16]. These three integrins, in particular, bind α5-laminins. The presence of the 7 most abundantly expressed integrins was additionally validated by qPCR from an additional batch of freshly isolated islets (Suppl. Fig. 5). To gain insight into receptors and laminin-induced signaling pathways in spreading islets, we plated mouse islets on LN-521, LN-421 or LN-111 for 3 and 12 days, and carried out RNA-seq to compare global transcriptomic changes induced by the different laminins (Fig. 3b, c). We found hundreds of differentially expressed (DE) genes between days 3 and 12 associated with different laminins (Suppl. Table 2). Notably, the LN-521 had a strong and specific effect on the islet transcriptome (resulting in 147 DE genes), in which the majority of genes were upregulated at day 12, as opposed to LN-111 and LN-421, where the majority of genes were downregulated (Fig. 3b). Consistent with the observed spreading of islets, functional annotation analysis of the upregulated genes associated with LN-521 revealed enrichment for KEGG pathways and molecular processes related to focal adhesion, extracellular matrix and cell-to-cell interaction (Fig. 3c, Suppl. Table 3). The transcriptomic analysis showed, for instance, that LN-521 induced a specific upregulation of the Thrombospondin 1 (*Thbs1*) gene, with a fold change (FC) of day 12 *vs* day 3 = 7.7, FDR = 5.6×10^{-52} (Suppl. Table 1), and the Connective Tissue Growth Factor-Related Protein 58/WNT1 Inducible Signaling Pathway Protein 2 (*Wisp2,* FC = 4.3, FDR = 5.2×10^{-10}) (Suppl. Table 1).

Characteristic hormone expression is maintained in islets cultured long-term on LN-521

In order to attain long-term survival of islets in culture (>14 days), we explored serum-free conditions together with LN-coating. Mouse islets plated on LN-521 could be cultured in a serum-free mTeSR1 medium for an extended period of time. The proportions of endocrine cells at day 14 were obtained by simultaneous staining for α-, β- and δ-cell markers (glucagon, C-peptide and somatostatin, respectively) (Fig. 4). On average, 65% of the islet cells stained positive for C-peptide (insulin). Glucagon-expressing α-cells also stained positive for insulin. These double-positive cells constituted on average 20% of the islet cells (Fig. 4). This pattern of double hormone expression was also observed for some α-cells in histological sections from mouse and monkey pancreata, while in both cases, δ-cells were shown to express somatostatin exclusively (Suppl. Fig. 6). During 21 days in culture, the islets expanded their area 6–17 fold when cultured on LN-521 (Fig. 5a, b), whereof spreading was most efficient for the first 5 days. In contrast, plating on Matrigel (includes LN-111) resulted in less efficient spreading during the first 5 days (~2 fold, Fig. 5b). To monitor proliferation in islets expanding on LN-521, we applied a 24 h pulse of EdU at different time points. Negligible proliferation was observed during the first two weeks (Fig. 4c, h, k: bright green EdU-AF488 labelled nuclei, appearing white). However, at day 17, extensive proliferation of islet cells was observed (Fig. 5c: red EdU-AF647 labelled nuclei). On average, 11% of the β-cells showed EdU incorporation at days 17–18 (Fig. 5c, d, e). Islets could be maintained on LN-521 for at least 35 days in serum-free conditions (Suppl. Fig. 7).

Discussion

Here, we describe a novel method to grow and maintain functional islets, from mouse and human, for at least seven days in culture. A key component of this method is the coating with biologically relevant laminins, found in the peri-islet capsule and BM of islet capillaries (Suppl. Fig. 1). Central necrosis of islets in suspension has previously been reported [17]. On LN-521 coated surfaces, whole islets can spread and thus, avoid the development of fatal hypoxia and necrosis, shown to occur in islets rapidly after isolation (Fig. 1c, Suppl. Fig. 2, Suppl. Videos 2a and b). Due to a diffusion barrier, larger islets are more vulnerable to hypoxia and therefore have a proportionally larger cell mass expelled (Suppl. Video 2b). This may partially explain the poor condition and the extensive number of human islets currently needed for transplantation. In contrast, islets expanded on LN-521 maintain functionality and glucose responsiveness, both *in vitro* (Fig. 1d, e) and *in vivo* (Fig. 2a, c). Our experiments in the STZ-induced T1D mouse model showed that transplantation of a small number of expanded islets was sufficient to rapidly achieve euglycemia. To our knowledge, 110 transplanted islets is the lowest amount sufficient to reverse chemically induced

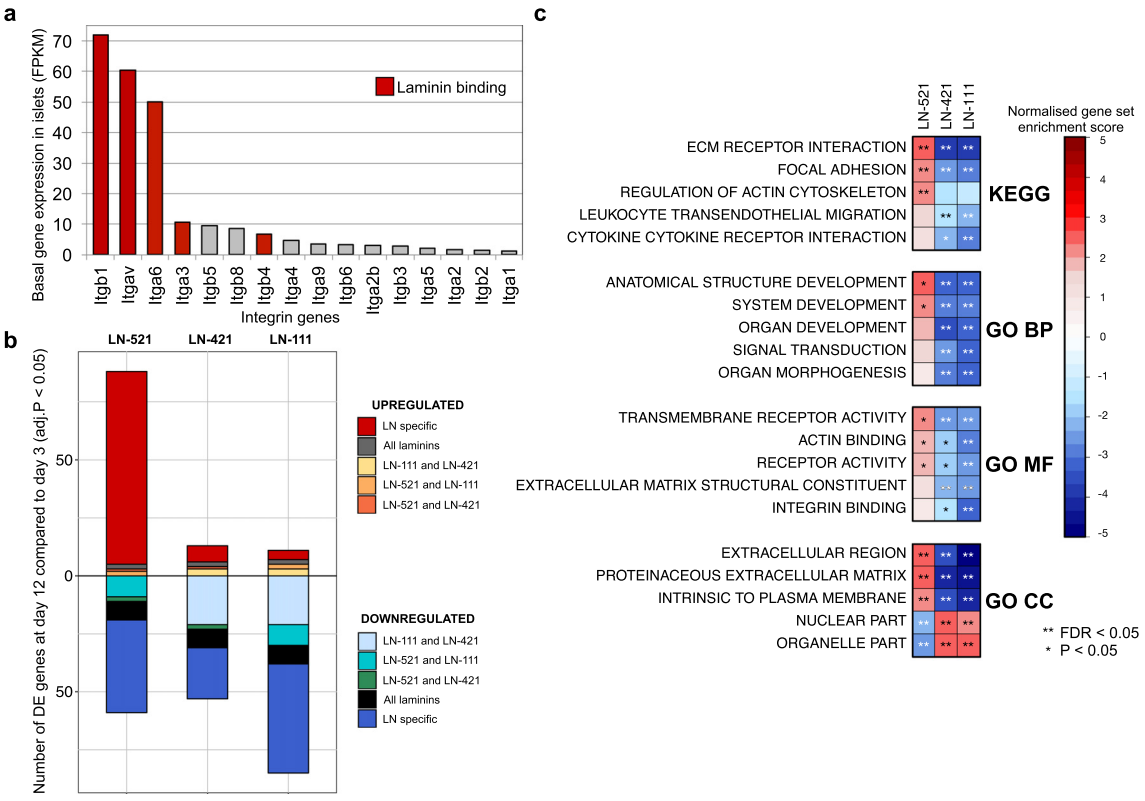

Fig. 3. LN-521 induces adhesion-specific transcriptomic signature in mouse islets. (a) Mean gene expression levels (Fragments Per Kilobase of transcript per Million, FPKM) of integrin genes with FPKM > 1 in isolated mouse islets (day 0, n = 3). Laminin-binding integrins (β1, αV, α6, α3 and β4) highlighted in red. Mean expression level of all integrin genes with the corresponding coefficient of variation listed in Suppl. Table 1. (b) Number of significantly differentially expressed genes with each laminin coating at day 12 compared to day 3 (Benjamini-Hochberg adjusted p-value < 0.05). (c) Top five functionally enriched KEGG pathways and GO terms from Gene Set Enrichment Analysis (GSEA) ranking the mouse genome by differential expression at day 12 *versus* day 3 with laminins (see Methods). Color mapped to GSEA normalized enrichment score (NES). The higher the NES value, the stronger the enrichment for the pathway that contains the upregulated genes. The lower the NES value, the stronger the enrichment for the pathway that contains the downregulated genes. Results sorted by LN-521 NES value. **significant results after multiple testing correction (GSEA FDR < 0.05). *nominally significant results (GSEA p < 0.05). Lack of (*) denotes non-significant results (GSEA p > 0.05).

diabetes in mice. Already within 3 days, 27% of the mice had reached normoglycemia, and 68% of the mice had normal glucose levels within a week (Fig. 2b). The low number of islets and the short time required for reaching euglycemia demonstrate the superiority of the spread islets compared to spherical islets in this transplantation setting [18]. Our data suggest that the flattened form of islets provides a significant rescue effect due to efficient oxygenation while in culture, and enables rapid vascularization post-transplantation. It has been reported that cultured, dispersed islet cells can be grown on LN-332 for 3 days [19–22]. In our

Fig. 4. Long-term islet cultures display characteristic hormone expression on LN-521. (a) Glucagon staining for α-cells (blue). (b) C-peptide staining (pro-insulin) for β-cells (red). (c) Somatostatin staining for δ-cells and EdU labelling of nuclei of proliferating cells (green). (d) Glucagon (blue) and insulin (red) merged. (e) Glucagon (blue) and somatostatin (green) merged. (f) Insulin (red) and somatostatin (green) merged. (g) Glucagon (blue), insulin (red) and somatostatin (green) merged. (h) Addition of Hoechst nuclei staining (cyan) to frame g. (i) Addition of mTomato fluorescence to frame h. (j) All isotype controls with corresponding secondary antibodies. (k) Addition of Hoechst nuclei staining (cyan) to frame j. (i) Addition of mTomato fluorescence to frame k. (m) In all, 23 monolayer islets (250–1100 cells/islet), were analyzed in Columbus, with results provided in (n). Crosses indicate average ± SEM. Images collected on Operetta applying a 20× NA objective. Scale bars 50 µm. Proliferation was measured by counting of EdU^+ nuclei (AF488: intensive green, appearing white). Such nuclei are indicated by arrows in frames c and h (a white arrow pointing to two endocrine nuclei, a yellow arrowhead pointing to a larger fibroblast nucleus).

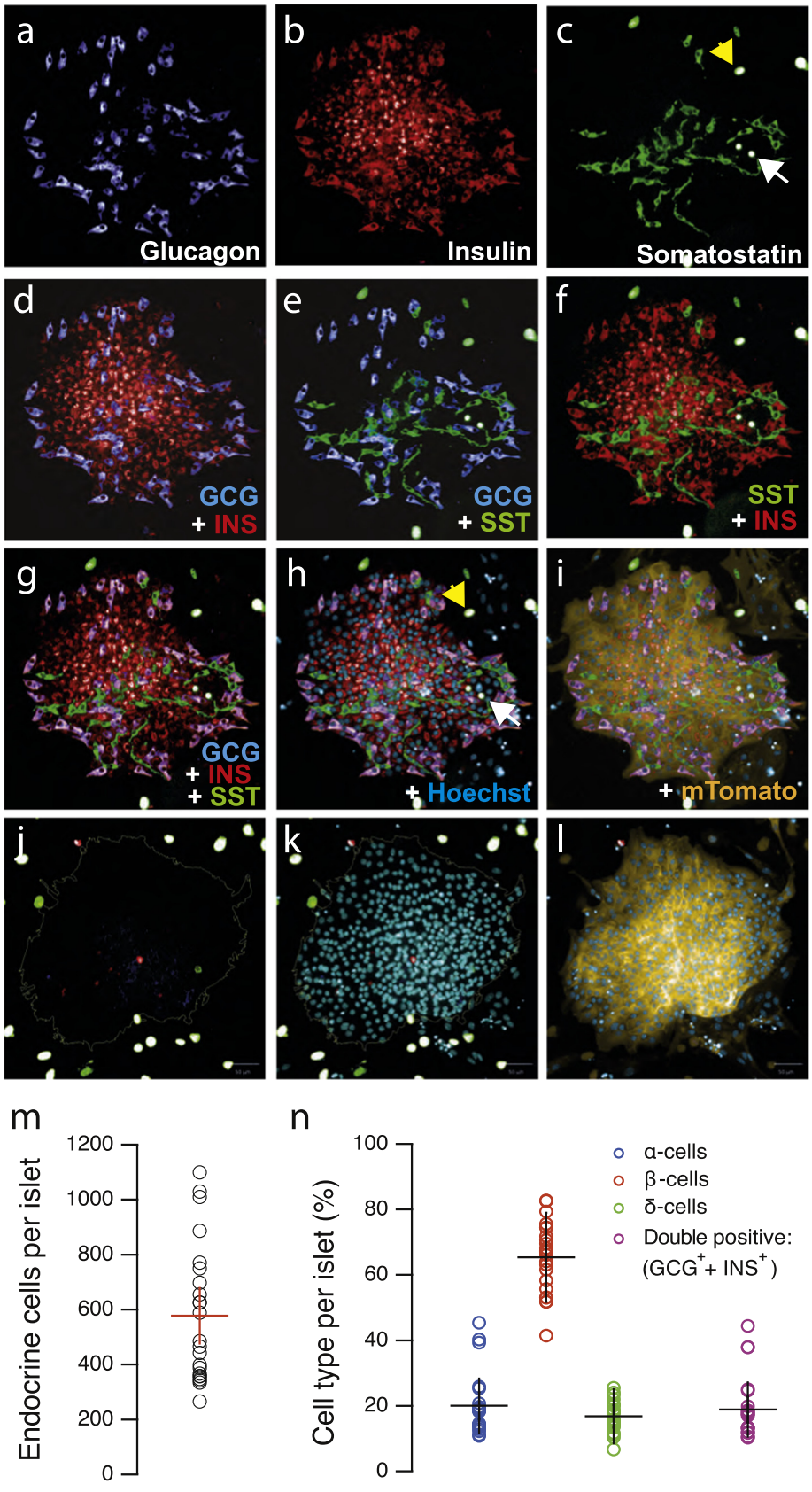

Fig. 4. (*legend on previous page*)

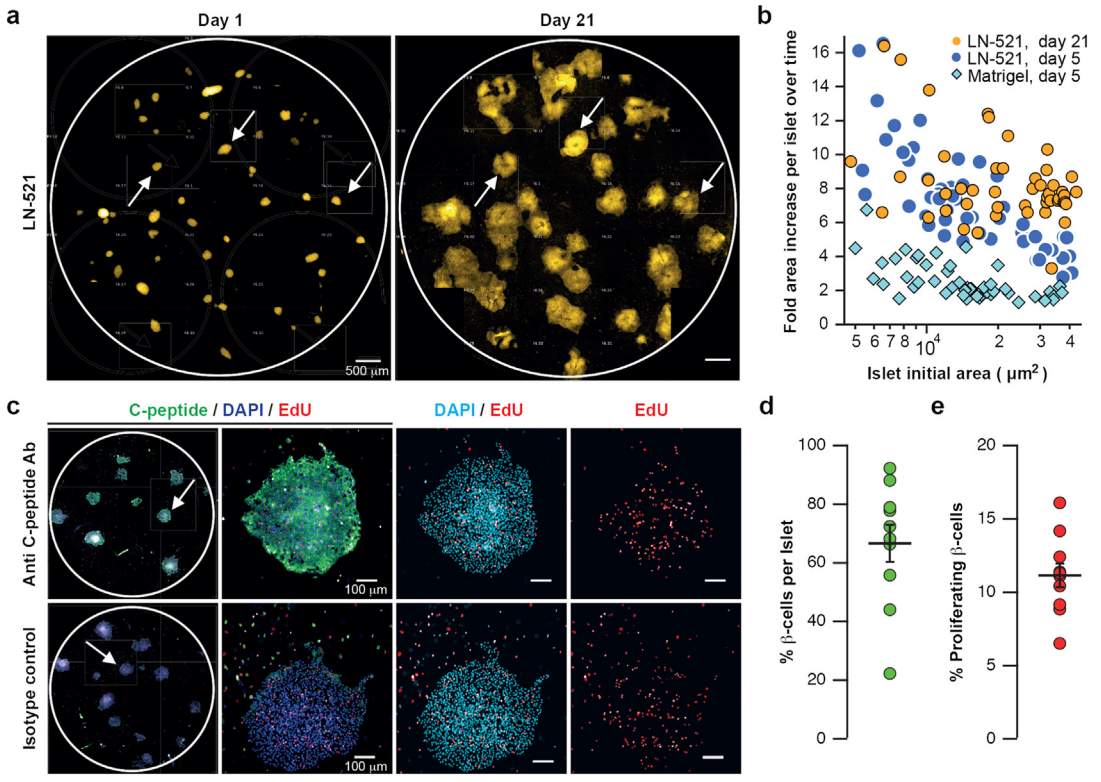

Fig. 5. LN-521 supports expansion and proliferation of mouse islets. (a) One microtiter well containing islets freshly plated on LN-521, followed from day 1 to day 21. Arrows depict comparison of the size of three identical islets. Scale bar 500 µm. (b) Expansion of islets plated on LN-521 compared to islets plated on Matrigel. (c) Islets grown for 18 days on LN-521, with EdU addition to medium for the last 24 h. Arrows point to a representative islet, provided in a higher magnification. Scale bar 100 µm. (d) All the islets in the two wells in c (n = 10 and n = 13) were analyzed at a single-cell level regarding nuclear morphology, EdU incorporation and the intensity of C-peptide staining. Results are plotted as mean ± SEM, providing % β-cells per islet and (e) % proliferating β-cells per islet; DAPI (blue/cyan) for nuclei, C-peptide (green) for β-cells, EdU-AF647 (red) for proliferating nuclei. Images were collected applying 10× and 20× objectives and quantified in Columbus.

study, islets on LN-332 showed initial spreading but subsequently underwent re-clustering with necrosis after 5 days (Fig. 1a). Additionally, we cultured islets on LN-411 and LN-421, which co-localize to islet capillaries [6,11] (Suppl. Fig. 1). However, following five days of spreading, cultures on these laminins also underwent re-clustering. Thus, α5-laminins appear to be critical for islet adhesion and long-term survival *in vitro*, indicating that islet homeostasis requires a specific matrix together with the appropriate receptors for induction of outside-in signaling. Our RNA-seq data showed that isolated mouse islets exhibit strong expression of α6- and β1-integrins, known to bind LN-511 and LN-521 [23]. In contrast, islet expression of α7-integrin (a major receptor for LN-111) was low (Suppl. Table 1). This may partially explain why islets do not bind efficiently to LN-111 coated surfaces. Here, comparative analysis of the transcriptomic changes of islets cultured on different laminins evidenced the distinctive beneficial effect of LN-521 on islet adhesion and spreading with up-regulation of extracellular matrix and attachment processes (Fig. 3b, c). The transcriptomic analysis also provided insights to genes potentially involved in laminin-mediated islet survival. THBS1 is a multifunctional protein with binding sites for several integrins. It has been shown to protect human and mouse β-cells against oxidative stress and cell death [24], and to promote angiogenesis in microvascular endothelia [25], which may benefit the survival of transplanted islets. WISP2 is an extracellular protein able to bind Insulin-like growth factor 1 and 2 [26]. It has binding sites for other ECM molecules and receptors, and plays a role in prevention of apoptosis *via* caspase-3 inhibition [27]. In order to prolong the *in vitro* survival of islets, we explored a variety of conditions, including serum-free cultures applying mTeSR1, which is commonly used for culturing pluripotent stem cells without feeder layer. Islets could be cultured for weeks in mTeSR1, with the characteristic hormone expression intact (Fig. 4). Approximately 20% of islet cells showed a co-expression of insulin and glucagon. The double-hormone expression was confirmed in histological

analyses of mouse and monkey pancreata (Suppl. Fig. 6). Simultaneous expression of glucagon and insulin in murine and human pancreatic cells has recently been reported [28–30]. It is debated whether such expression is implicated in β-cell trans-differentiation, as shown by Kornete et al. [31]. Alternatively, these cells might represent a pool of not yet fully differentiated, or slightly de-differentiated cells. Recently, Blodgett et al. identified high levels of insulin mRNA in purified adult human glucagon-expressing α-cells [32]. Together, these data indicate the need to revise the dogma on exclusive hormone expression pattern of islet endocrine cells. Thus, the current method of defining cell types applying a single marker selection in single-cell RNA-seq studies might need to be re-evaluated [32–34]. One major aim of the islet research has been to identify compounds that can stimulate islet cell proliferation and thereby increase β-cell mass. It has been shown that inhibition of GSK3B and DYRKIA can induce human β-cell replication [35,36] and overexpression of Nkx6.1 and Pdx-1 leads to islet cell proliferation [37]. Several other factors such as PAX4, Wnt3A and PDGF-AA have been reported to stimulate proliferation of immature β-cells, but not of adult islet cells [38–40]. Recently, Phelps et al. [41] published a Y-27632 (a ROCK-inhibitor) based protocol providing 16% proliferation in cultures of embryonic rat islets. About 6% and over 30% proliferation of β-cells have been documented from applying, notably, a 4 days pulse of EdU combined with the DYRK1A inhibitor GNF4877, on primary β-cell cultures from human and young rats, respectively [35]. In this study, the flattened islets start robust cell proliferation after a lag period of approximately two weeks in a serum-free mTeSR1 culture on LN-521. It should be mentioned that mTeSR1 contains $[Li^+] = 1$ mM. Lithium is known to provide an inhibitory effect on amino acid- and glucose-induced insulin secretion by mechanisms involving microtubular fusion and calcium influx in pancreatic β-cells [42], and in agreement with this, we observed that islets in this medium lose their physiological response to glucose. Nevertheless, mouse islets grown in serum-free medium on LN-521 showed significant proliferation around day 18, with 11% of EdU^+ β-cells following a 24 h EdU pulse, with no inhibitors or stimuli added (Fig. 5c, e).

The results of this study indicate that human islets can be flattened in the same manner as for mouse. The possibility to use such well-oxygenated and functional islets could significantly increase the efficacy of future islet transplantations. Furthermore, given the small number of transplanted islets sufficient to achieve normoglycemia and superior glucose control, our protocol could decrease the need for multiple donors and provide ample time for HLA typing and elective surgery. Finally, our novel method could also ameliorate the transplantation of autologous islets from patients with T2D or pancreatic cancer undergoing partial pancreatectomy.

Methods

Study design

The objective of this study was to evaluate which laminin isoform would provide the best support to culture mammalian islets and to characterize the effects of laminin on islet survival, functionality and proliferation. Different laminin matrices were tested multiple times with mouse and human islets. Glucose stimulated insulin secretion *in vitro* was carried out at least twice with size-sorted islets. Islet transplantation to diabetic mice was performed three times in independent cohorts with glucose tolerance test conducted with the largest cohort. Samples for RNA sequencing were randomized to three batches at the time of RNA isolation. Long-term cultures were conducted in serum-free conditions, and immunohistochemistry and EdU-based proliferation assays were performed in triplicate wells.

Experimental animals

C57Bl/6N mice of age 8–12 weeks were used for streptozotocin-induced type 1 diabetes (T1D) and as controls for glucose tolerance test. For transplantation, islets were isolated either from C57Bl/6N or B6·Cg-Tg(CAG-DsRed * MST)1Nagy/J mice. For *in vitro* studies, male C57Bl/6N or mTomato/mGFP mice (B6.129(Cg)-Gt(ROSA)26Sortm4(ACTB-tdTomato-EGFP)Luo/J, Jackson Laboratory, stock n:o 007676) of age 5–8-weeks expressing mTomato in cell membranes, were used as islet donors for all experiments. Food and water were supplied *ad libitum*. All procedures were performed according to ethical permits issued by the local Ethical Committee at Karolinska Institutet, Stockholm, and the IACUC committee at Duke-NUS Medical School, Singapore.

Mouse islet isolation, selection and sorting

For islet functional analyses and transplantation experiments, islets were isolated and manually sorted as previously described [43,44]. Pancreata were perfused with 1 mg/ml Collagenase XI (Sigma) in HBSS buffer (with Ca^{2+} and Mg^{2+}) and incubated at 37 °C for 10–15 min with gentle shaking. The islets in suspension were dispersed, washed and collected on 100 µm meshes. Islets for GSIS experiments were handpicked and plated according to size (small: 70–100 µm, medium:100–150 µm, and large: 150–250 µm).

Extracellular matrix coatings

We used human recombinant laminins LN-521, LN-511, LN-421, LN-411, LN-111, LN-121, LN-332 (BioLamina AB, Sweden), mouse EHS-sarcoma

derived LN-111 (Invitrogen) and growth factor reduced Matrigel (BD Biosciences). Laminins were diluted 1:3 in PBS for the culture plate coating, and 1:5 in HBSS for the PDMS membrane coating. 96- and 384-well microtiter plates (PerkinElmer) were coated, incubated at 37 °C for 1 h, and washed 3 times with PBS buffer to remove unbound molecules.

Mouse islet culturing

Culture medium either contained serum or was serum-free. The media contained 10% fetal calf serum in RPMI1640 (50%) (Invitrogen) and CMRL1066 (50%) (Corning), with 10 mM HEPES, 1% Glutamax, and 1% Penicillin/Streptomycin. Long-term cultures were conducted with serum-free, chemically defined mTeSR1 medium (StemCell), containing 4 mM glucose and 1% Penicillin/Streptomycin. The islets were cultured in 200 µl of media in 96-well microtiter plates at 5% CO_2, 37 °C. Half of the media was changed every 2 days.

Human islets

Human islets were purchased from Prodo Laboratories Inc. (California), and transferred in Prodo Laboratories Inc.'s medium. After arrival, the islets were plated in a medium containing 10% human AB serum (PIM(ABS), Prodo Laboratories Inc.) in CMRL1066 (Corning) with 1% supplement (PIM(G), Prodo Laboratories Inc.), 1% HEPES, 1% pyruvate, 1% transferrin, and 1% Penicillin/Streptomycin. The islets were cultured in 200 µl of medium at 5% CO_2, 37 °C with half of the media changed every 2–3 days.

Glucose stimulated insulin secretion (GSIS)

Isolated mouse islets from mTomato mice were handpicked by size in serum-containing media. Ten small and medium size islets, and five large islets were plated as triplicates in 96-well culture plates (Corning) coated with LN-521. Ten medium sized human islets were plated per well (n = 5) and cultured for seven days. The GSIS assay was performed with a medium consisting of RPMI1640, 2% BSA, 1% HEPES, 1% Glutamax, 1% Penicillin/Streptomycin, and glucose concentrations were adjusted to 2 mM, 8 mM or 25 mM. Prior to the start of the experiment, islets were washed with 8 mM glucose medium to eliminate traces of serum. Islets were first incubated with 2 mM glucose medium for 1 h, followed by 25 mM glucose medium for 1 h, and finally with 8 mM glucose medium for 1 h. The media were collected after each incubation step, spun for 1 min (1000 rpm) and supernatants were frozen at -30 °C for insulin ELISA assay (Millipore, EZRMI-13 K). Samples were diluted 20× and run according to manufacturer's protocol.

Membrane and barrier production

Silastic MDX4-4210 BioMedical Grade Elastomer (Dow Corning) was prepared in a 1:10 (w/w) ratio of curing agent to elastomer and degassed. Films of elastomer were prepared by spin coating at 1500 rpm for 30 s on 100 mm silicon wafers and cured at 120 °C for 15 min, resulting in membranes 140 ± 10 µm thick. The cured membranes were washed in 70% (v/v) ethanol three times, and oxygen plasma treated for 5 min at 300 mTorr (Harrick Plasma). The surface was treated for 2 h with a 5% (v/v) solution of (3-aminopropyl) triethoxysilane (APTES) (Sigma Aldrich) prepared in 95% ethanol at pH 4.5. Excess APTES was removed by washing three times with 95% (v/v) ethanol and condensed at 110 °C for 60 min under vacuum. Treated membranes were cut into 12 mm discs, affixed to dry 6-well plates and sterilized in 70% ethanol. Barriers (Suppl. Fig. 4a) with 6 mm outer diameter (OD) and 4 mm inner diameter (ID) inner ring nested within an outer ring of 14 mm OD × 6 mm ID were prepared from Sylgard 184 Silicone Elastomer (Dow Corning) cast in 2 mm thick sheets, degassed under vacuum, and cured for 72 h at room temperature. Barriers were sterilized in 70% ethanol and stacked on top of the APTES-treated membranes placed in culture plates.

Streptozotocin-induced mouse model of T1D and islet transplantation

For the generation of STZ-induced diabetic mice, 8–10 weeks-old C57Bl/6N mice were fasted for 4–6 h prior to STZ-injection [12–14]. STZ (Sigma) was dissolved in freshly prepared citrate buffer (100 mM citric acid, pH 4.5) to a concentration of 22.5 mg/ml immediately prior to injection. The mice received a single i.p. injection (160–165 mg/kg). The blood glucose was measured twice per week using a glucometer (Contour, Bayer, Germany). Mice with non-fasted glucose levels of at least 22 mM were selected for transplantation experiments.

For transplantation treatment, medium-size islets were cultured for 3 or 7 days on PDMS membranes treated with APTES and coated overnight with 50 µl of LN-521 (30 µg/ml) in a well of a culture plate. The laminin coating area was 4 mm in diameter (Suppl. Fig. 4a). Two 5 mm diameter membranes, each containing 55–75 islets, were stanched out and transplanted beneath the kidney capsule. Non-fasted blood glucose was measured daily the first 3 days, and later twice a week. Islet-transplanted kidneys were removed for immunohistochemical analysis 8 weeks post-operation. Blood glucose was monitored for one additional week in order to determine that normoglycemia was achieved due to the transplanted islets. For the null-graft control group, STZ-treated male mice (n = 4) were transplanted with PDMS membranes devoid of islets. As these mice remained severely hyperglycemic and

kept losing weight, they were euthanized three weeks post-operation.

Intraperitoneal glucose tolerance test (IPGTT)

Six weeks post-transplantation, C57Bl/6N male mice (total n = 9) were fasted for 6 h, weighed and injected i.p. with 10% D-glucose (1 mg/g body weight). Blood glucose was measured at 7, 15, 30, 60, 90 and 120 min post-injection. Non-operated 10-week-old C57Bl/6N male mice (n = 7) were used as controls.

Imaging and cell population quantification

For live cell imaging of islets spreading on coated surfaces, islets form 8–10 weeks-old C57Bl/6N or mTomato mice, or a human donor, were plated on 96w CellCarrier microtiter plates (PerkinElmer) in mTeSR1 supplemented with 4 mM glucose. Initial spreading of islets from C57Bl/6N mice was followed by time-laps applying bright field imaging, every 15 min spanning from 12 to 62 h after plating (Suppl. Videos 1a, b) on an Operetta microscope (PerkinElmer) at 5% CO_2 and 37 °C. Subsequently, the spreading of human islets was followed by bright field imaging once per day (Fig. 1b).

Islet surface area quantification

Fluorescence images were applied to measure the increase of surface area of mTomato islets during spreading. Initial areas were calculated from images collected 1 h after plating, and compared with images collected at later time points. To analyze individual islets within each well, images were stitched using the Columbus software (PerkinElmer) whereafter islet areas were quantified using ImageJ [45]. For live imaging of hypoxia and necrosis, islets were pre-stained with Hoechst 33342 (0.5 μM) (Sigma, cat# B2261) and DRAQ7 (1 μM) (BioStatus), starting 1 h *a priori*, in mTeSR1 supplemented with 4 mM glucose. Subsequently, the hypoxia marker MAR (1 μM) (Goryo Chemical, Inc.) was added, followed by time-lapse imaging for 72 h, with image collection every 2 h. During pre-incubation and imaging, samples were kept at 37 °C and 5% CO_2.

Immunocytochemistry analysis

Islet cultures were fixed with 4% PFA for 20 min at RT, washed three times with PBS and treated with 0.5% Triton-X in PBS, pH 7.5 for 15 min. For analysis of the transplanted islets, the operated kidneys were fixed with 4% PFA overnight at +4 °C. The engrafted Actin-DsRed red fluorescent islets were identified and a thin slice of the kidney parenchyma was excised for whole mount staining. The tissue was permeabilized for 3 × 30 min at RT with PBS containing 1% Triton X-100, 0,1 mM $CaCl_2$, 0,1 mM $MgCl_2$, and 0,1 mM $MnCl_2$. The samples were blocked overnight in the same buffer containing 1% BSA and then incubated overnight with primary antibodies in the blocking buffer, washed 3 × 2 h and incubated with secondary antibodies overnight. The washed samples were mounted and analyzed on a Zeiss LSM700 confocal microscope. The antibodies used to stain for laminin chains in monkey islets (Suppl. Fig. 1) have been previously described [46]. Detailed information of antibodies is provided in Suppl. Table 4. Proliferation was assayed using Click-iT EdU Alexa Fluor-488 or Alexa Fluor-647 imaging kit (Invitrogen, #C10337). Image collection of mTomato islets was performed using Operetta applying 10×, 20×, and 40× objectives. Images were analyzed with Columbus (PerkinElmer).

RNA isolation and RNA-seq

Mouse islets were isolated, handpicked and medium-sized islets were plated into 24-well plates coated with LN-111, LN-421 or LN-521. Twenty islets/well were plated in triplicates on each laminin coatings and cultured 0, 3 or 12 days. The serum-containing medium was changed every third day. On defined days, islets were collected and stored in RNAlater® (Invitrogen) prior to RNA isolation. Total RNA was isolated from islets collected from each of the three wells (A, B and C), time points (day 0, 3 and 12) and laminin coatings (LN-111, LN-421 and LN-521) with Single-cell RNA isolation kit (Norgen Biotek) according to manufacturer's protocol. In total, 21 samples were processed. RNA quantity and quality were measured using Bioanalyzer instrument with Agilent Pico RNA 6000 kit (Agilent Technologies). RNA-Seq libraries were constructed with 2 ng of total RNA using Ovation® Single-Cell RNA-Seq System (NuGEN, part no. 0342). Barcoded libraries were multiplexed and sequenced as paired-end 75 bp reads on Illumina HiSeq2000 platform in three batches. RNA-seq data have been deposited at the Gene Expression Omnibus database (accession number GSE89677).

Processing of RNA-seq data

The quality of the sequencing reads was ascertained *via* FASTQC tool (http://www.bioinformatics.babraham.ac.uk/projects/fastqc). Average sequencing depth was 113.3 million reads per sample and the median per-base quality was >30 for all the samples. No further trimming of the bases was performed. Sequencing reads were mapped to the mouse reference genome (mm10) using STAR alignment tool (version 2.5.1b) [47]. Only uniquely mapped reads were reported from STAR by setting the parameter—outFilterMulrimapNmax 1. The mean mapping rate was 86.1% and the mean rRNA mapping rate was 33.4%. Fragments Per Kilobase of transcript per Million mapped reads (FPKM) and gene counts were

computed with Cufflinks (version 2.1.1) [48]. From Cufflinks outputs, only genes with status "OK" were selected in every sample. Missing values (corresponding to Cufflinks status "FAIL", 23 values in total) were imputed by using the function pca from the R package pcaMethods (version 1.60.0) [49]. This data imputation was performed in both FPKM and gene raw counts expression matrices separately by setting the nPcs parameter to the number of samples (n = 21). Thereafter, gene counts were rounded using the R function round.

Differential expression and pathway enrichment

Differential expression (DE) was computed at the gene level with the imputed rounded gene counts using DESeq2 R package (version 1.10.1) [49]. For each set of samples treated with the same laminin coating, one DE run was performed comparing the gene expression profiles at day 12 with day 3 (n = 3 for each laminin coating and time point). The base comparison was set to day 3 in all the runs. The technical covariates "sequencing batch" and "RIN score" were added as covariates in the differential_expression model. DESeq2 function results was run by setting the cooksCutoff parameter to False and the independentFiltering parameter to False. The rest of the parameters were left as default. In further analyses, Log2 fold changes computed by DESeq2 are always considered. Results of the DE analysis are provided in Suppl. Table 1.

Pathway functional enrichment of the DE results was performed with Gene Set Enrichment Analysis (GSEA) software (version gsea2-2.2.2) [50]. Mouse genes with mean DESeq2 normalized counts for all samples higher than 0 were selected (DESeq2 output baseMean >0). Mouse Ensembl gene IDs were mapped to human Ensembl gene IDs by retrieving one-to-one orthologs from Ensembl (Ensembl version 83, using biomaRt R package, version 2.26.1) [51]. Human Ensembl genes IDs were then mapped to HGNC symbols by retrieving "hgnc_symbol" (also using biomaRt R package and the same Ensembl version). Once all mouse genes were mapped to their corresponding human orthologs, these were ranked by the corresponding DESeq2 output Wald statistic ("stat", defined as estimate of the Log2 fold change divided by its standard error) from each of the three DE runs (*e.g.* LN-521 on day 12 *versus* LN-521 on day 3). Three functional GSEA runs were performed (one for each DE test) assessing overrepresentation of Gene Ontology (GO) and Kyoto Encyclopedia of Genes and Genomes (KEGG) pathways derived from the Molecular Signatures Database gene sets (v5.1, gene sets queried using gene symbols) [50]. GSEA was run in classic pre-rank mode with 10,000 permutations to assess the false discovery rate (FDR). In the GSEA runs, maximum cluster size was set to 5000 and minimum to 10. The top five enriched KEGG and GO terms were selected and represented in a graph (Fig. 3c). To generate this graph the top enriched terms were defined selecting those categories enriched after multiple testing correction (FDR < 0.05) by the following hierarchy: 1) take terms enriched in all three laminin coatings, 2) add those enriched in only LN-521, 3) add the terms enriched in both LN-421 and LN-111 and 4) add terms enriched in either LN-421 or LN-111. Thereafter, the five terms with the strongest enrichment (represented by Normalized Enrichment Score, NES) were selected. Full list of results is provided in Suppl. Table 2.

qPCR

Total RNA (550 ng) was reverse-transcribed to cDNA applying TaqMan Reverse Transcription Reagents (Applied Bioystems). TaqMan probes (Thermofisher) were purchased and qPCR was performed using the ABI OneStep Plus Real-Time PCR System (Applied Biosystems). Triplicate for each sample was carried out. The relative quantification of gene expression was analyzed using the comparative threshold (Ct) method, using mouse GAPDH as an endogenous control for RNA load and gene expression. The difference in Ct-values (ΔCt) between the target gene and the reference gene was calculated, and the ΔCt's were compared directly.

Statistical analysis

Groups in IPGTT were compared applying 2-tailed Student's *t*-test, and samples in GSIS by pair-wise, 2-tailed Student's *t*-test. $p < 0.05$ was defined as significant.

Data availability

All data are available within the paper and its supplementary information, or are available from the Gene Expression Omnibus database under accession code GSE89677 for RNA-seq data.

Supplementary data to this article can be found online at https://doi.org/10.1016/j.matbio.2018.03.018.

Acknowledgments

We are grateful to the staff of the Duke-NUS Genome Biology Facility for running RNA-seq samples and to animal husbandry staff Carin Sandberg and Matilda Andrae at the Department's animal facility at Karolinska Institutet. We thank Prof. Ralph Bunte at Duke-NUS Medical School for his assistance with non-human primate samples, and Asst. Prof. Gianluca Grenci and Ms. Sree Vaishnavi

Sundararajan at the Mechanobiology Institute of the National University of Singapore for helping with the treatment of PDMS membranes. This work was supported in part by grants from the National Medical Research Council, Singapore (NMRC/STaR/010/2012 (KT), CBRG15may062 (EP) and WBS R913200076263 (SG)), Swedish Cancer Society (MP), Vetenskapsrådet, Sweden (KT, MP, MMS), Diabetesfonden, Sweden (KT) and Diabetes Research & Wellness Foundation (2749/2014SW), Sweden (KT).

Author contributions

K.S., J.R.M.O., M.K.Ö., A-M.Ö., A.D, S.R. and A-S.N. carried out islet isolation and culturing of mammalian islets. K.S. did imaging and image analyses. B.G. wrote ImageJ macro for islet area quantification. M.K.Ö. isolated mRNA and constructed the libraries for RNA-seq. A-M.Ö. performed qPCR analysis. The sequencing data were annotated and analyzed by A.M-M., X.C., S.G. and E.P. L.Y.C. carried out immunostaining of tissues. J.A.M.S. and M.M.S. provided the PDMS membranes used for transplantation. J.R.M.O., M.K.Ö., A.D. and A-M.Ö. carried out transplantation experiments. Mouse colony management was done by M.K.Ö. Genotyping was carried out by M.K.Ö. and Y.S. M.P. provided monoclonal laminin antibodies. K.T. conceived the study, designed and wrote the manuscript together with K.S., A-M.Ö., M.K.Ö., J.R.M.O., A.D., A.M.-M. and E.P.

Competing financial interests

K.T. and S.R. are shareholders in BioLamina AB.

Received 24 January 2018;
Received in revised form 22 March 2018;
Accepted 22 March 2018
Available online 27 March 2018

Keywords:
Diabetes;
Laminin;
Pancreatic;
Islet;
Transplantation;
β-cell

†Equal contribution.
‡Equal contribution.

§Current address: Division of Transplantation Surgery, Department of Clinical Science, Intervention and Technology, Karolinska Institutet, Stockholm, Sweden.

||Current address: Division of Chemistry I, Department of Medical Biochemistry & Biophysics, Karolinska Institutet, Stockholm, Sweden.

Abbreviations used:
T1D, type 1 diabetes; BM, basement membrane; LN, laminin; ECM, extracellular matrix; GSIS, glucose stimulated insulin secretion; PDMS, polydimethylsiloxane; STZ, streptozotocin; IPGTT, intraperitoneal glucose tolerance test; DE, differentially expressed.

References

[1] D.M. Harlan, N.S. Kenyon, O. Korsgren, B.O. Roep, Immunology of diabetes, current advances and travails in islet transplantation, Diabetes 58 (10) (2009) 2175–2184.
[2] M.D. Bellin, F.B. Barton, A. Heitman, J.V. Harmon, R. Kandaswamy, A.N. Balamurugan, D.E. Sutherland, R. Alejandro, B.J. Hering, Potent induction immunotherapy promotes long-term insulin independence after islet transplantation in type 1 diabetes, Am. J. Transplant. 12 (6) (2012) 1576–1583.
[3] R.W. Gruessner, A.C. Gruessner, The current state of pancreas transplantation, Nat. Rev. Endocrinol. 9 (9) (2013) 555–562.
[4] C.C. Center, Collaborative Islet Transplant Registry Annual Report 2012 In: C.I.T. Registry (Ed.) National Institute of Diabetes & Digestive & Kidney Diseases, National Institutes of Health, Bethesda, MD, 2014.
[5] R. Lehmann, R.A. Zuellig, P. Kugelmeier, P.B. Baenninger, W. Moritz, A. Perren, P.A. Clavien, M. Weber, G.A. Spinas, Superiority of small islets in human islet transplantation, Diabetes 56 (3) (2007) 594–603.
[6] A. Domogatskaya, S. Rodin, K. Tryggvason, Functional diversity of laminins, Annu. Rev. Cell Dev. Biol. 28 (2012) 523–553.
[7] P.D. Yurchenco, Basement membranes: cell scaffoldings and signaling platforms, Cold Spring Harb. Perspect. Biol. 3 (2) (2011).
[8] A. Pozzi, P.D. Yurchenco, R.V. Iozzo, The nature and biology of basement membranes, Matrix Biol. 57-58 (2017) 1–11.
[9] M.A. Gubbiotti, T. Neill, R.V. Iozzo, A current view of perlecan in physiology and pathology: a mosaic of functions, Matrix Biol. 57–58 (2017) 285–298.
[10] G. Nikolova, N. Jabs, I. Konstantinova, A. Domogatskaya, K. Tryggvason, L. Sorokin, R. Fassler, G. Gu, H.P. Gerber, N. Ferrara, D.A. Melton, E. Lammert, The vascular basement membrane: a niche for insulin gene expression and Beta cell proliferation, Dev. Cell 10 (3) (2006) 397–405.
[11] I. Virtanen, M. Banerjee, J. Palgi, O. Korsgren, A. Lukinius, L. E. Thornell, Y. Kikkawa, K. Sekiguchi, M. Hukkanen, Y.T. Konttinen, T. Otonkoski, Blood vessels of human islets of Langerhans are surrounded by a double basement membrane, Diabetologia 51 (7) (2008) 1181–1191.
[12] M.C. Deeds, J.M. Anderson, A.S. Armstrong, D.A. Gastineau, H.J. Hiddinga, A. Jahangir, N.L. Eberhardt, Y. C. Kudva, Single dose streptozotocin-induced diabetes: considerations for study design in islet transplantation models, Lab. Anim. 45 (3) (2011) 131–140.
[13] A.A. Like, A.A. Rossini, Streptozotocin-induced pancreatic insulitis: new model of diabetes mellitus, Science 193 (4251) (1976) 415–417.

[14] N. Rakieten, M.L. Rakieten, M.V. Nadkarni, Studies on the diabetogenic action of streptozotocin (NSC-37917), Cancer Chemother. Rep. 29 (1963) 91–98.
[15] T. Bock, B. Pakkenberg, K. Buschard, Genetic background determines the size and structure of the endocrine pancreas, Diabetes 54 (1) (2005) 133–137.
[16] M. Barczyk, S. Carracedo, D. Gullberg, Integrins, Cell Tissue Res. 339 (1) (2010) 269–280.
[17] M. Giuliani, W. Moritz, E. Bodmer, D. Dindo, P. Kugelmeier, R. Lehmann, M. Gassmann, P. Groscurth, M. Weber, Central necrosis in isolated hypoxic human pancreatic islets: evidence for postisolation ischemia, Cell Transplant. 14 (1) (2005) 67–76.
[18] M. McCall, R. Pawlick, T. Kin, A.M. Shapiro, Anakinra potentiates the protective effects of etanercept in transplantation of marginal mass human islets in immunodeficient mice, Am. J. Transplant. 12 (2) (2012) 322–329.
[19] K. Ohashi, S. Mukobata, R. Utoh, S. Yamashita, T. Masuda, H. Sakai, T. Okano, Production of islet cell sheets using cryopreserved islet cells, Transplant. Proc. 43 (9) (2011) 3188–3191.
[20] T. Saito, K. Ohashi, R. Utoh, H. Shimizu, K. Ise, H. Suzuki, M. Yamato, T. Okano, M. Gotoh, Reversal of diabetes by the creation of neo-islet tissues into a subcutaneous site using islet cell sheets, Transplantation 92 (11) (2011) 1231–1236.
[21] H. Shimizu, K. Ohashi, R. Utoh, K. Ise, M. Gotoh, M. Yamato, T. Okano, Bioengineering of a functional sheet of islet cells for the treatment of diabetes mellitus, Biomaterials 30 (30) (2009) 5943–5949.
[22] S. Yamashita, K. Ohashi, R. Utoh, T. Okano, M. Yamamoto, Human laminin isotype coating for creating islet cell sheets, Cell Med. 8 (1–2) (2015) 39–46.
[23] H. Yu, J.F. Talts, Beta1 integrin and alpha-dystroglycan binding sites are localized to different laminin-G-domain-like (LG) modules within the laminin alpha5 chain G domain, Biochem. J. 371 (Pt 2) (2003) 289–299.
[24] D.A. Cunha, M. Cito, P.O. Carlsson, J.M. Vanderwinden, J.D. Molkentin, M. Bugliani, P. Marchetti, D.L. Eizirik, M. Cnop, Thrombospondin 1 protects pancreatic beta-cells from lipotoxicity via the PERK-NRF2 pathway, Cell Death Differ. 23 (12) (2016) 1995–2006.
[25] I. Staniszewska, S. Zaveri, L. Del Valle, I. Oliva, V.L. Rothman, S.E. Croul, D.D. Roberts, D.F. Mosher, G.P. Tuszynski, C. Marcinkiewicz, Interaction of alpha9beta1 integrin with thrombospondin-1 promotes angiogenesis, Circ. Res. 100 (9) (2007) 1308–1316.
[26] S. Kumar, A.T. Hand, J.R. Connor, R.A. Dodds, P.J. Ryan, J. J. Trill, S.M. Fisher, M.E. Nuttall, D.B. Lipshutz, C. Zou, S.M. Hwang, B.J. Votta, I.E. James, D.J. Rieman, M. Gowen, J.C. Lee, Identification and cloning of a connective tissue growth factor-like cDNA from human osteoblasts encoding a novel regulator of osteoblast functions, J. Biol. Chem. 274 (24) (1999) 17123–17131.
[27] S. Chowdhury, X. Wang, C.B. Srikant, Q. Li, M. Fu, Y.J. Gong, G. Ning, J.L. Liu, IGF-I stimulates CCN5/WISP2 gene expression in pancreatic beta-cells, which promotes cell proliferation and survival against streptozotocin, Endocrinology 155 (5) (2014) 1629–1642.
[28] H. Chakravarthy, X. Gu, M. Enge, X. Dai, Y. Wang, N. Damond, C. Downie, K. Liu, J. Wang, Y. Xing, S. Chera, F. Thorel, S. Quake, J. Oberholzer, P.E. MacDonald, P.L. Herrera, S.K. Kim, Converting adult pancreatic islet alpha cells into beta cells by targeting both Dnmt1 and Arx, Cell Metab. 25 (3) (2017) 622–634.
[29] J. Li, T. Casteels, T. Frogne, C. Ingvorsen, C. Honore, M. Courtney, K.V. Huber, N. Schmitner, R.A. Kimmel, R.A. Romanov, C. Sturtzel, C.H. Lardeau, J. Klughammer, M. Farlik, S. Sdelci, A. Vieira, F. Avolio, F. Briand, I. Baburin, P. Majek, F.M. Pauler, T. Penz, A. Stukalov, M. Gridling, K. Parapatics, C. Barbieux, E. Berishvili, A. Spittler, J. Colinge, K.L. Bennett, S. Hering, T. Sulpice, C. Bock, M. Distel, T. Harkany, D. Meyer, G. Superti-Furga, P. Collombat, J. Hecksher-Sorensen, S. Kubicek, Artemisinins target GABAA receptor signaling and impair alpha cell identity, Cell 168(1–2) (2017) 86–100 e15.
[30] T. van der Meulen, A.M. Mawla, M.R. DiGruccio, M.W. Adams, V. Nies, S. Dolleman, S. Liu, A.M. Ackermann, E. Caceres, A.E. Hunter, K.H. Kaestner, C.J. Donaldson, M.O. Huising, Virgin beta cells persist throughout life at a neogenic niche within pancreatic islets, Cell Metab. 25 (4) (2017) 911–926 (e6).
[31] M. Kornete, H. Beauchemin, C. Polychronakos, C.A. Piccirillo, Pancreatic islet cell phenotype and endocrine function throughout diabetes development in non-obese diabetic mice, Autoimmunity 46 (4) (2013) 259–268.
[32] D.M. Blodgett, A. Nowosielska, S. Afik, S. Pechhold, A.J. Cura, N.J. Kennedy, S. Kim, A. Kucukural, R.J. Davis, S.C. Kent, D.L. Greiner, M.G. Garber, D.M. Harlan, P. diIorio, Novel observations from next-generation RNA sequencing of highly purified human adult and fetal islet cell subsets, Diabetes 64 (9) (2015) 3172–3181.
[33] N. Lawlor, J. George, M. Bolisetty, R. Kursawe, L. Sun, S. V, I. Kycia, P. Robson, M.L. Stitzel, Single cell transcriptomes identify human islet cell signatures and reveal cell-type-specific expression changes in type 2 diabetes, Genome Res. 27 (2) (2017) 208–222.
[34] Y. Xin, J. Kim, H. Okamoto, M. Ni, Y. Wei, C. Adler, A.J. Murphy, G.D. Yancopoulos, C. Lin, J. Gromada, RNA sequencing of single human islet cells reveals type 2 diabetes genes, Cell Metab. 24 (4) (2016) 608–615.
[35] W. Shen, B. Taylor, Q. Jin, V. Nguyen-Tran, S. Meeusen, Y. Q. Zhang, A. Kamireddy, A. Swafford, A.F. Powers, J. Walker, J. Lamb, B. Bursalaya, M. DiDonato, G. Harb, M. Qiu, C.M. Filippi, L. Deaton, C.N. Turk, W.L. Suarez-Pinzon, Y. Liu, X. Hao, T. Mo, S. Yan, J. Li, A.E. Herman, B.J. Hering, T. Wu, H. Martin Seidel, P. McNamara, R. Glynne, B. Laffitte, Inhibition of DYRK1A and GSK3B induces human beta-cell proliferation, Nat. Commun. 6 (2015) 8372.
[36] P. Wang, J.C. Alvarez-Perez, D.P. Felsenfeld, H. Liu, S. Sivendran, A. Bender, A. Kumar, R. Sanchez, D.K. Scott, A. Garcia-Ocana, A.F. Stewart, A high-throughput chemical screen reveals that harmine-mediated inhibition of DYRK1A increases human pancreatic beta cell replication, Nat. Med. 21 (4) (2015) 383–388.
[37] H.L. Hayes, L. Zhang, T.C. Becker, J.M. Haldeman, S.B. Stephens, M. Arlotto, L.G. Moss, C.B. Newgard, H.E. Hohmeier, A Pdx-1-regulated soluble factor activates rat and human islet cell proliferation, Mol. Cell. Biol. 36 (23) (2016) 2918–2930.
[38] T. Brun, I. Franklin, L. St-Onge, A. Biason-Lauber, E.J. Schoenle, C.B. Wollheim, B.R. Gauthier, The diabetes-linked transcription factor PAX4 promotes {beta}-cell proliferation and survival in rat and human islets, J. Cell Biol. 167 (6) (2004) 1123–1135.
[39] H. Chen, X. Gu, Y. Liu, J. Wang, S.E. Wirt, R. Bottino, H. Schorle, J. Sage, S.K. Kim, PDGF signalling controls age-dependent proliferation in pancreatic beta-cells, Nature 478 (7369) (2011) 349–355.

[40] I.C. Rulifson, S.K. Karnik, P.W. Heiser, D. ten Berge, H. Chen, X. Gu, M.M. Taketo, R. Nusse, M. Hebrok, S.K. Kim, Wnt signaling regulates pancreatic beta cell proliferation, Proc. Natl. Acad. Sci. U. S. A. 104 (15) (2007) 6247–6252.
[41] E.A. Phelps, C. Cianciaruso, J. Santo-Domingo, M. Pasquier, G. Galliverti, L. Piemonti, E. Berishvili, O. Burri, A. Wiederkehr, J.A. Hubbell, S. Baekkeskov, Advances in pancreatic islet monolayer culture on glass surfaces enable super-resolution microscopy and insights into beta cell ciliogenesis and proliferation, Sci. Rep. 7 (2017), 45961.
[42] J.H. Anderson Jr., W.G. Blackard, Effect of lithium on pancreatic islet insulin release, Endocrinology 102 (1) (1978) 291–295.
[43] D.S. Li, Y.H. Yuan, H.J. Tu, Q.L. Liang, L.J. Dai, A protocol for islet isolation from mouse pancreas, Nat. Protoc. 4 (11) (2009) 1649–1652.
[44] N.D. Stull, A. Breite, R. McCarthy, S.A. Tersey, R.G. Mirmira, Mouse islet of Langerhans isolation using a combination of purified collagenase and neutral protease, J. Vis. Exp. (67) (2012).
[45] C.A. Schneider, W.S. Rasband, K.W. Eliceiri, NIH image to ImageJ: 25 years of image analysis, Nat. Methods 9 (7) (2012) 671–675.
[46] T. Ishikawa, Z. Wondimu, Y. Oikawa, S. Ingerpuu, I. Virtanen, M. Patarroyo, Monoclonal antibodies to human laminin alpha4 chain globular domain inhibit tumor cell adhesion and migration on laminins 411 and 421, and binding of alpha6beta1 integrin and MCAM to alpha4-laminins, Matrix Biol. 36 (2014) 5–14.
[47] A. Dobin, C.A. Davis, F. Schlesinger, J. Drenkow, C. Zaleski, S. Jha, P. Batut, M. Chaisson, T.R. Gingeras, STAR: ultrafast universal RNA-seq aligner, Bioinformatics 29 (1) (2013) 15–21.
[48] C. Trapnell, A. Roberts, L. Goff, G. Pertea, D. Kim, D.R. Kelley, H. Pimentel, S.L. Salzberg, J.L. Rinn, L. Pachter, Differential gene and transcript expression analysis of RNA-seq experiments with TopHat and Cufflinks, Nat. Protoc. 7 (3) (2012) 562–578.
[49] W. Stacklies, H. Redestig, M. Scholz, D. Walther, J. Selbig, pcaMethods—a bioconductor package providing PCA methods for incomplete data, Bioinformatics 23 (9) (2007) 1164–1167.
[50] A. Subramanian, P. Tamayo, V.K. Mootha, S. Mukherjee, B. L. Ebert, M.A. Gillette, A. Paulovich, S.L. Pomeroy, T.R. Golub, E.S. Lander, J.P. Mesirov, Gene set enrichment analysis: a knowledge-based approach for interpreting genome-wide expression profiles, Proc. Natl. Acad. Sci. U. S. A. 102 (43) (2005) 15545–15550.
[51] S. Durinck, P.T. Spellman, E. Birney, W. Huber, Mapping identifiers for the integration of genomic datasets with the R/Bioconductor package biomaRt, Nat. Protoc. 4 (8) (2009) 1184–1191.